Acta Crystallographica Section D
Biological Crystallography
ISSN 0907-4449

Apocrustacyanin C_1 crystals grown in space and on earth using vapour-diffusion geometry: protein structure refinements and electron-density map comparisons

Jarjis Habash,[a] Titus J. Boggon,[a] James Raftery,[a] Naomi E. Chayen,[b] Peter F. Zagalsky[c] and John R. Helliwell[a]*

[a]Section of Structural Chemistry, Department of Chemistry, University of Manchester, Manchester M13 9PL, England, [b]Biological Structure and Function Section, Division of Biomedical Sciences, Faculty of Medicine, Imperial College London, SW7 2AZ, England, and [c]Department of Molecular Biology and Biochemistry, Royal Holloway College, University of London, Egham, Surrey TW20 0EX, England

Correspondence e-mail: john.helliwell@man.ac.uk

Received 22 January 2003
Accepted 8 April 2003

PDB References: apocrustacyanin C_1, space-grown, 1obq, r1obqsf; apocrustacyanin C_1, earth-grown, 1obu, r1obusf.

We dedicate this paper to all the astronauts who risk their lives in pushing forward the frontiers of microgravity science and discovery, and of human exploration, and especially to all the crew of the 2002 Columbia Space Shuttle Mission who died on the final step of their return to earth.

Models of apocrustacyanin C_1 were refined against X-ray data recorded on Bending Magnet 14 at the ESRF to resolutions of 1.85 and 2 Å from a space-grown and an earth-grown crystal, respectively, both using vapour-diffusion crystal-growth geometry. The space crystals were grown in the APCF on the NASA Space Shuttle. The microgravity crystal growth showed a cyclic nature attributed to Marangoni convection, thus reducing the benefits of the microgravity environment, as reported previously [Chayen *et al.* (1996), *Q. Rev. Biophys.* **29**, 227–278]. A subsequent mosaicity evaluation, also reported previously, showed only a partial improvement in the space-grown crystals over the earth-grown crystals [Snell *et al.* (1997), *Acta Cryst.* D**53**, 231–239], contrary to the case for lysozyme crystals grown in space with liquid–liquid diffusion, *i.e.* without any major motion during growth [Snell *et al.* (1995), *Acta Cryst.* D**52**, 1099–1102]. In this paper, apocrustacyanin C_1 electron-density maps from the two refined models are now compared. It is concluded that the electron-density maps of the protein and the bound waters are found to be better overall for the structures of apocrustacyanin C_1 studied from the space-grown crystal compared with those from the earth-grown crystal, even though both crystals were grown using vapour-diffusion crystal-growth geometry. The improved residues are on the surface of the protein, with two involved in or nearby crystal lattice-forming interactions, thus linking an improved crystal-growth mechanism to the molecular level. The structural comparison procedures developed should themselves be valuable for evaluating crystal-growth procedures in the future.

1. Introduction

Protein crystal growth in the microgravity environment of space has been advocated as an attractive option owing to the absence or near-absence of convection and sedimentation (Littke & John, 1984; Walter, 1987). Gradually, it has been shown that macromolecular crystals grown in space may indeed be larger and more perfect, *i.e.* with a lower mosaicity and a better reflection intensity signal to noise ratio, and may even diffract to higher resolution (Koszelak *et al.*, 1995; Snell *et al.*, 1995; Chayen, Boggon *et al.*, 1996; McPherson, 1997; Borgstahl *et al.*, 2001; Kundrot *et al.*, 2001; Vergara *et al.*, 2003).

However, we also found only a 'partial' improvement of crystal quality for microgravity-grown apocrustacyanin C_1 crystals (Snell *et al.*, 1997). The crystal perfection of five crystals (three from space and two from earth) was evaluated *via* a comparison of mosaicity plotted against reflection signal to noise ratio. The diffraction quality of one space-grown apocrustacyanin C_1 crystal was the best, a crystal pair from

space and earth were as good as each other, and the other pair were as poor as each other. These different results were suggested to be attributable to crystal movement during growth in microgravity owing to the use of vapour diffusion and it was suggested that Marangoni convection may have induced the cyclic motion in the drops (Chayen, Boggon *et al.*, 1996).

In evaluating crystals from space, more recent attention has focused on the quality of the protein model itself and of the bound solvent. Dong *et al.* (1999) observed improvement in the bound-solvent structure for a lysozyme crystal grown in space. Very recently, Ng *et al.* (2002) showed that the aminoacyl-tRNA synthetase structure from a space-grown crystal was more accurate, had better defined amino-acid side chains and better order of the bound water molecules. In another study of phenolic insulin crystals grown in microgravity, Smith *et al.* (1996) showed significant changes in the conformations of side chains in the vicinity of a binding site and that several side chains existed in more than a single discrete conformation.

The work presented in this paper involves refinement of the model of apocrustacyanin C_1 using a space-grown crystal and an earth-grown crystal, from the crystal-growth experiments on the LMS mission (Chayen, Boggon *et al.*, 1996; Boggon *et al.*, 1998), with X-ray data recorded at ESRF on a bending magnet to resolutions of 1.85 and 2 Å, respectively. Electron-density maps are also truncated to 2 Å and both the protein and the bound solvent are examined residue by residue and water by water to observe the effects of the absence of gravity during crystal growth. Finally, the study was extended further for the purpose of comparison of the space-grown and earth-grown crystals by using only the common reflections between the two data sets to 2 Å resolution.

2. Crystallization

The apocrustacyanin C_1 was purified by Dr P. F. Zagalsky and crystallized by Dr N. E. Chayen. The protocols used were as described previously (Chayen, Gordon *et al.*, 1996; Chayen *et al.*, 1997; Snell *et al.*, 1997). The space crystals were grown in the Advanced Protein Crystallization Facility (APCF) on board the Space Shuttle during the Life and Microgravity Spacelab (LMS) mission and as ground controls using the vapour-diffusion method in the same type of apparatus. A crystal was picked from a space reactor and one from a ground control reactor. This structural comparison study followed mosaicity and topography evaluations (Boggon, 1998) which thus restricted choice especially for the ground control where fewer of the bigger crystals were available.

3. Data collection and data reduction

Single-crystal X-ray diffraction data sets were measured on the microgravity-grown crystal and the ground-control crystal of apocrustacyanin C_1 (Boggon, 1998); both crystals were mounted in quartz capillaries. The data-collection X-ray source was beamline BM14 of the ESRF tuned to a wavelength of 0.7513 Å; diffraction data were recorded on a CCD detector at room temperature. Cryoconditions were not used, even though these were likely to help improve the diffraction resolution in each case, as these would introduce the chance of variation between the crystals. Instead, by keeping both the crystals at room temperature this opportunity for variability was avoided.

Table 1
Data-collection protocol and data-reduction statistics for microgravity and ground-control apocrustacyanin C_1.

	Microgravity	Ground control
Crystal dimensions (mm)	1.20 × 0.24 × 0.15	0.80 × 0.07 × 0.06
Crystal volume (mm^3)	0.0432	0.0034
Beam size (µm)	150 × 150	150 × 150
Maximum illuminated crystal volume (mm^3)	0.0054	0.0006
Oscillation range per image (°)	1	1
Crystal-to-detector distance (mm)	150	150
Exposure time per image (s)	30	30
Total rotation (°)	135	135
Wavelength (Å)	0.7513	0.7513
Resolution† (Å)	25–2.0	25–2.0
$\langle I\rangle/\langle\sigma(I)\rangle$ all data (outer shell)	30.4 (7.7)	9.5 (1.4)
Total No. of measurements	160645	163297
No. of unique data	24764	26098
Completeness (%)	94.7	99.2
$R_{\rm merge}$	0.056	0.110

† Data are truncated to 25–2 Å resolution for the purpose of comparison; the space data extended to 1.85 Å.

Data were processed and merged using the *HKL* suite (Otwinowski, 1993; Otwinowski & Minor, 1997). Apocrustacyanin C_1 crystallizes in space group $P2_12_12_1$, with unit-cell parameters for the space crystal and earth crystal of a = 41.959, b = 80.539, c = 110.649 Å and a = 42.018, b = 81.033, c = 110.507 Å, respectively. Table 1 gives the details of data collection, with data reduction in the range 25–2 Å shown for ease of comparison of the two data sets.

4. Molecular structure

Apocrustacyanin C_1 crystallizes with a homodimer (362 residues) in the asymmetric unit; the subunit has 181 amino-acid residues (Gordon *et al.*, 2001) with molecular weight 20 kDa. Its homologue apocrustacyanin A_1 has two post-translational modifications Asp5→Asn and Leu181→Val (Cianci *et al.*, 2001). Both A_1 and C_1 belong to the carotenoproteins which are responsible for colouration of marine crustacea. For example, the blue colour of the lobster carapace is associated with the binding of astaxanthin molecules to an A_1–A_3 protein dimer (for details, see Cianci *et al.*, 2002).

5. Structure refinement using all data for the space and earth crystals

The apocrustacyanin C_1 structures were refined to 1.85 Å resolution for the space and 2 Å resolution for the earth case. The atomic coordinates for the starting model were taken from the Protein Data Bank (PDB code 1i4u; Gordon *et al.*, 2001) determined at 1.15 Å resolution using data collected on

Table 2
Final parameters for refinements.

	Space, 1.85 Å	Earth, 2 Å	Space, 2 Å (common)	Earth, 2 Å (common)
Resolution range high (Å)	1.85	2	2	2
Resolution range low (Å)	64.55	65.94	24	24
Data cutoff	None	None	None	None
Completeness (%)	87	99.2	94.2	94.2
No. of reflections	27216	24728	23324	23324
Free *R* value test-set size (%)	5.1	5.1	5.1	5.1
Free *R* value test-set count	1450	1326	1266	1266
No. of non-H atoms used in refinement	3069	3059	3019	3023
Mean *B* value (Å^2)	19.3	19.0	20.0	20.3
Bond lengths, refined atoms (r.m.s.) (Å)	0.028	0.034	0.032	0.035
Bond angles, refined atoms (r.m.s.) (°)	2.2	2.5	2.3	2.5
Torsion angles (r.m.s.) (°)	5.3	5.7	5.6	5.9
Ramachandran plot statistics†				
Residues in most favoured regions (%)	91.9	91.9	92.5	92.5
Residues in additional allowed regions (%)	6.9	6.5	6.5	6.5
Residues in generously allowed regions (%)	0.6	0.9	0.3	0.3
Residues in disallowed regions‡ (%)	0.6	0.6	0.6	0.6
PDB codes	1obq	1obu	—	—

† Calculated using *PROCHECK*; the rest of the values were determined using *REFMAC*5 (both from the *CCP*4 program suite). ‡ These are residues Tyr112*A* and *B* and are as noted previously in the structural analysis of Cianci *et al.* (2001).

an ESRF undulater insertion device at cryotemperature. The existing waters were removed and a new water structure was determined.

5.1. Apocrustacyanin C_1 crystal grown in space

Rigid-body refinement (*REFMAC*5; Collaborative Computational Project, Number 4, 1994) was performed on the molecule at 1.85 Å. After five cycles of refinement, the overall *R* factor, free *R* factor and overall figure of merit converged to 0.295, 0.295 and 0.767, respectively. Following this, the *DDQ* (Difference Density Quality) program (Akker & Hol, 1999) was used. This procedure yielded 116 water molecules.

The refinement was then extended with the structure undergoing restrained refinement with temperature factors refined isotropically for five cycles; the overall *R* factor, free *R* factor and overall figure of merit converged to 0.185, 0.215 and 0.845, respectively. *DDQ* was again used to determine and update the new water structure to 149 water molecules.

Electron-density maps were calculated using the *FFT* program, which is also part of the *CCP*4 suite, and were displayed on a Silicon Graphics system using the *O* program (Jones *et al.*, 1991). The model generally fitted the $2F_o - F_c$ electron-density map well and was inspected at a contour level of 1 r.m.s., but residues Asn*A*18, Lys*A*61, Phe*A*101, Asn*B*29, Phe*B*101 and Asp*B*144 were remodelled to fit the electron density, and Lys*B*61 was extended from C^β to the full side chain. In both chains *A* and *B*, a total of 21 and 22 side-chain residues, respectively, appeared either with partly fragmented density or partly without density, and this was corroborated by the exhibition of high temperature factors for those atoms. The three disulfide bridges for each monomer of the molecule (Cys12–Cys121, Cys51–Cys173 and Cys117–Cys150) were well formed, with bond lengths of 2.05, 2.01 and 2.00 Å, respectively, for chain *A,* and of 2.01, 1.98 and 2.00 Å, respectively, for chain *B*.

The structure was refined for one more iteration and the water molecules were then checked; after deletion of 11 waters that encroached on each other, a further iteration of refinement was carried out. 18 waters were added and Lys*A*61 and Asn*B*29 were remodelled. The final statistics were overall *R* factor 0.169, free *R* factor 0.210 and overall figure of merit 0.853. The final structure contained 156 water molecules with 130 waters common with the earth structure (see next section); the final parameters for this refinement are shown in Table 2.

To test whether any bias might have been involved in starting with the 1i4u model, the above procedure was repeated but applying random shifts to the atoms (∼0.25 Å) and the refinement steps were repeated. This test led to essentially indistinguishable electron-density maps. [In order to start from the same coordinates, random shifts to the 1i4u model were not made in the subsequent refinements below.]

5.2. Apocrustacyanin C_1 crystal grown on earth

The same refinement procedure was used as in the previous subsection to a data resolution limit of 2 Å. Residues Lys*A*11, Asn*A*18, Phe*A*101, Phe*B*101, Asp*B*144 and Gln*B*145 were remodelled to fit the electron density and Lys*B*61 was extended from C^β to full side chain. In chains *A* and *B*, a total of 23 and 26 side-chain residues, respectively, appeared with either partly fragmented density or partly without density and this was corroborated by high temperature factors for these atoms. The final model had an overall *R* factor of 0.174, a free *R* factor of 0.227 and an overall figure of merit of 0.830. The model contained 146 water molecules and the final parameters for this refinement are shown in Table 2.

6. Structure refinement using common reflections for the space and earth data

As mentioned above, the apocrustacyanin C_1 crystal grown in space diffracted to 1.85 Å resolution, while its counterpart the earth-grown crystal diffracted to 2 Å resolution. The space data set was now cut to 2 Å resolution and only common reflections with the earth data were kept to control for Fourier series truncation errors. The $R_{\rm free}$ subset was thereby identical for each case. The completeness of the common reflection set is 94.2%. Since the earth data to 2 Å resolution have a completeness of 99.2%, the space data set is the set largely responsible for those reflections that are missing. The values of $\langle F\rangle$, $\langle {\rm sd}\rangle$, $\langle F\rangle/\langle {\rm sd}\rangle$ and $\langle F/{\rm sd}\rangle$ were 242.43, 7.84, 30.90 and 39.32 and 234.62, 20.40, 11.50 and 19.71, respectively, for the space and earth cases for the common data.

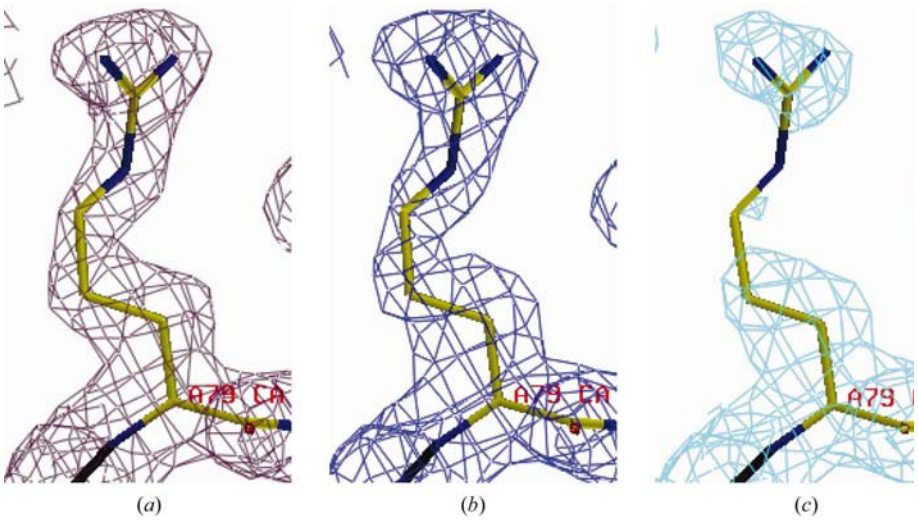

Figure 1
Section of $2F_o - F_c$ protein electron-density map showing Arg*A*79 at 1 r.m.s. contour level: (*a*) space data at 1.85 Å resolution, (*b*) space data at 2 Å resolution, for which the density is better, (*c*) earth data at 2 Å resolution. The map correlation coefficient for the side chain is 0.97 for (*a*) and (*b*), and 0.91 for (*a*) and (*c*).

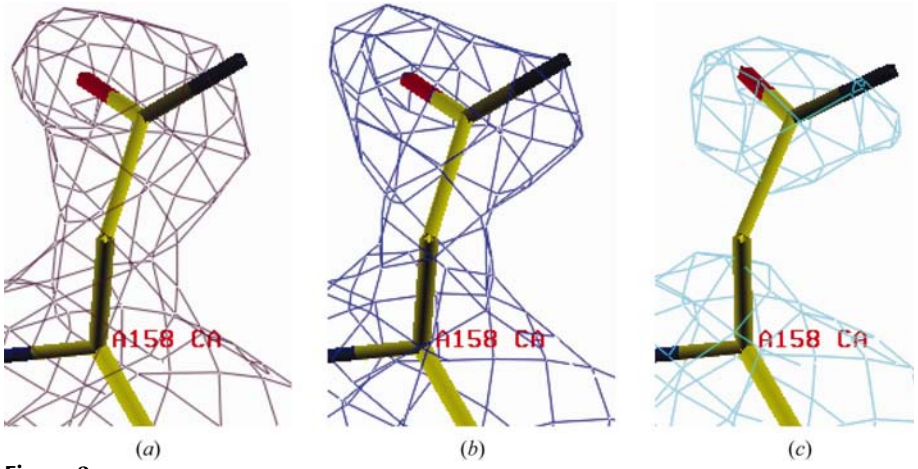

Figure 2
Section of $2F_o - F_c$ protein electron-density map showing Asn*A*158 at 1 r.m.s. contour level: (*a*) space data at 1.85 Å resolution. (*b*) space data at 2 Å resolution, for which the density is better, (*c*) earth data at 2 Å resolution. The map correlation coefficient for the side chain is 0.96 for (*a*) and (*b*), and 0.80 for (*a*) and (*c*).

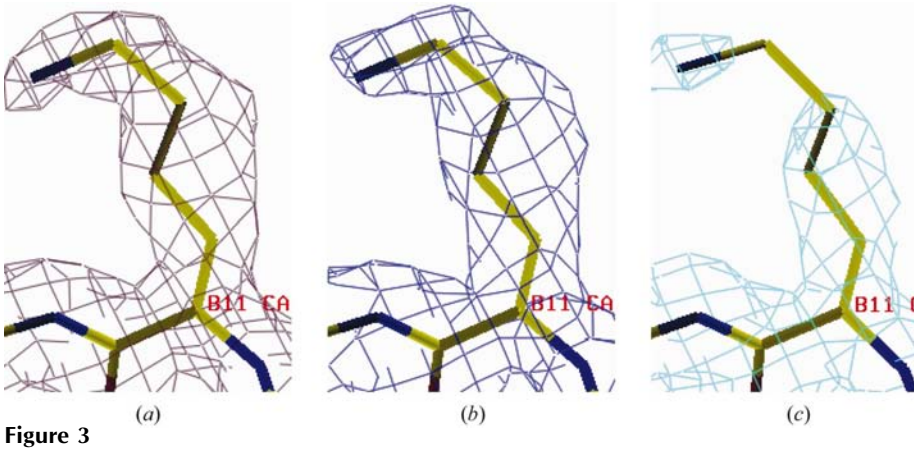

Figure 3
Section of $2F_o - F_c$ protein electron-density map showing Lys*B*11 at 1 r.m.s. contour level: (*a*) space data at 1.85 Å resolution,. (*b*) space data at 2 Å resolution, for which the density is better, (*c*) earth data at 2 Å resolution. The map correlation coefficient for the side chain is 0.97 for (*a*) and (*b*), and 0.89 for (*a*) and (*c*).

6.1. Apocrustacyanin C_1 crystal grown in space

The refinement of the model basically followed the same procedure and used the same computer programs as described earlier. Residues Asn*A*18, Phe*A*101, Asn*B*29 and Phe*B*101 were remodelled. The final overall *R* factor, free *R* factor and overall figure of merit converged to 0.179, 0.211 and 0.843, respectively, and the model contained 110 water molecules, with 104 waters common with the earth structure (see §6.2). The final parameters for this refinement are shown in Table 2.

6.2. Apocrustacyanin C_1 crystal grown on earth

The refinement followed the same procedure and used the same computer programs as described earlier. Residues Asn*A*18, Phe*A*101, Asn*B*29 and Phe*B*101 were remodelled. The final overall *R* factor, free *R* factor and overall figure of merit converged to 0.184, 0.214 and 0.842, respectively, and the model contained 114 water molecules. The final parameters for this refinement are shown in Table 2.

7. Results

7.1. Space and earth structures using all data

7.1.1. The protein electron densities. The final models and the representative protein electron densities of the two structures from space and earth were superimposed and visually compared in a residue-by-residue search using *O* on a Silicon Graphics System using a contour level of 1 r.m.s. for the $2F_o - F_c$ electron-density maps and 2σ for the difference electron-density $F_o - F_c$ maps. Each chain (*A* and *B*) of the molecule has 181 amino acids, but residue 1 is not visible in chain *B*.

In chain *A*, 132 residues appeared nearly the same in density, 34 residues looked better in the space case and 15 looked better in the earth case. In chain *B*, 149 residues appeared nearly the same, 19 residues looked better in the space case and 12 looked better in the earth case. The best examples of the effect on the electron densities are

shown in Figs. 1, 2 and 3 (a full suite of these figures is available as supplementary material[1]). Additional electron density of the space crystal to full data at 1.85 Å resolution is also shown.

7.1.2. The water structure. The structure from the space crystal has 156 bound water molecules, whereas the structure from the earth crystal has 146 bound water molecules (130 in common). Following the same procedure implemented in the comparison of the protein residues in §7.1.1, 62 waters appeared nearly the same in density, 47 waters looked better in the space crystal and 21 waters looked better in the earth crystal. Examples of the densities are shown in Figs. 4 and 5.

7.1.3. Space and earth structures using common reflections. The same method of comparison of the previous subsections (§7.1) was used. Seven residues looked better in the space structure (Asp*A*1, Lys*A*2, Lys*A*19, Arg*A*79, Lys*B*2, Arg*B*28 and Glu*B*90 with map correlation coefficients *versus* the 1.85 Å resolution of 0.95, 0.94; 0.81, 0.76; 0.89, 0.87; 0.93, 0.91; 0.80, 0.74; 0.92, 0.90 and 0.94, 0.92; space, earth, respectively). See Figs. 6 and 7. None were better in the earth structure. In the water structure seven waters looked better in the space structure and one looked better in the earth case.

Interestingly, all four data sets show the key water equivalent to that bound to a keto oxygen of each astaxanthin in the β-crustacyanin structure.

8. Discussion and conclusions

The four protein models are clearly very similar overall; the r.m.s. deviations between the coordinate sets are given in Table 3. Given the factor of 9 difference in crystal volumes this is quite remarkable. Set against these structural similarities there are, however, differences in some of the structural details. In the comparison study of the space and earth crystals using all the data available, 77.8% of the residues looked nearly the same in the electron density, 14.7% looked better in the space case and 7.5% looked better in the earth case.

As for the water structure, the effect of microgravity was more pronounced. This is in agreement with Dong *et al.* (1999) and Ng *et al.* (2002). Specifically, here 47.7% of the waters looked nearly the same in their electron density, 36.1% looked better in the space case and 16.1% looked better in the earth crystal case. Using common reflections, seven residues and seven waters in the space structure looked better, with the earth showing one better water only, while most of the protein and the waters looked closely similar. As Table 4 shows, when using the common reflections, the average *B* factor for the protein and the common waters is slightly more favourable for the space

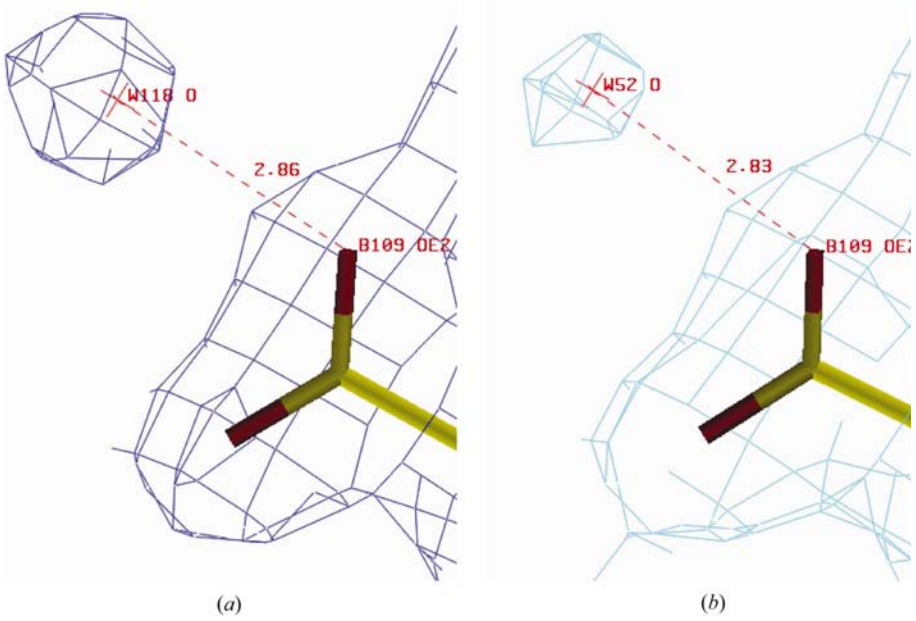

Figure 4
Section of $2F_o - F_c$ protein electron-density map showing an equivalent water at 1 r.m.s. contour level: (*a*) space data (water 118), for which the density is better, (*b*) earth data (water 52).

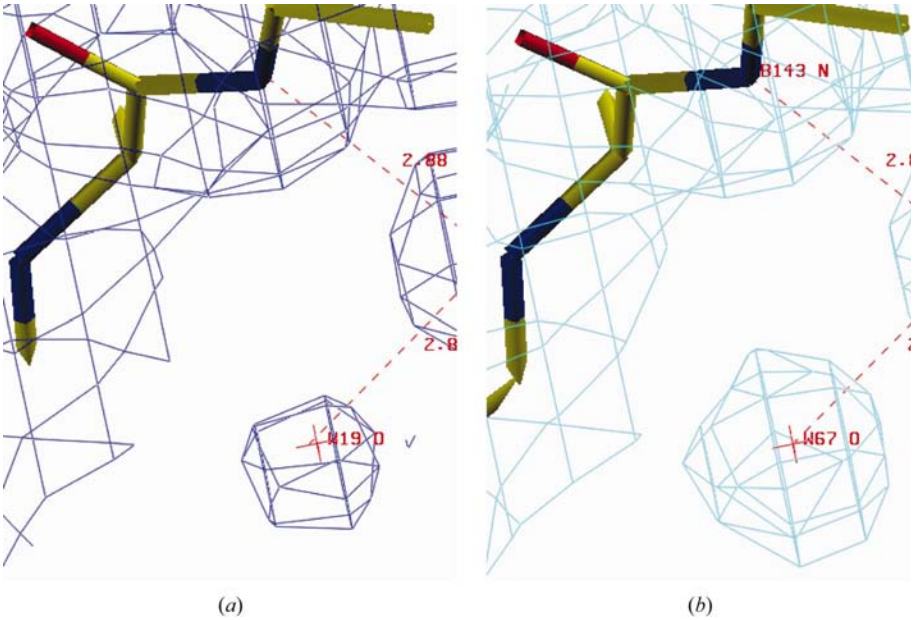

Figure 5
Section of $2F_o - F_c$ protein electron-density map showing an equivalent water at 1 r.m.s. contour level: (*a*) space data (water 19), (*b*) earth data (water 67), for which the density is better.

[1] Supplementary material has been deposited in the IUCr electronic archive (Reference: en0080). Details for accessing this material are described at the back of the journal.

crystal (21.5 and 26.3 Å^2, respectively) compared with the earth crystal (21.8 and 27.2 Å^2, respectively).

The amino-acid side chains showing improved electron density should be involved in the crystal lattice-forming interactions. Two of these amino-acid side chains (Asp*A*1 and Lys*A*2) are involved in or nearby crystal lattice-forming interactions; the other five, whilst on the protein surface, are not obviously involved in that way (see Fig. 7). Nevertheless, to see improved side-chain density on the protein surface and at a crystal lattice contact is a logical connection between the molecular level and crystal-growth mechanisms.

Overall, these observations of the electron-density comparisons, along with the atomic *B*-factor values, suggest slight improvements have accrued from the use of microgravity, even though the use of vapour-diffusion geometry in microgravity may have caused Marangoni convection-driven motion of the growing crystals (Chayen, Boggon *et al.*, 1996), which is not ideal The structural comparison procedures developed should themselves be valuable for evaluating crystal-growth procedures in the future.

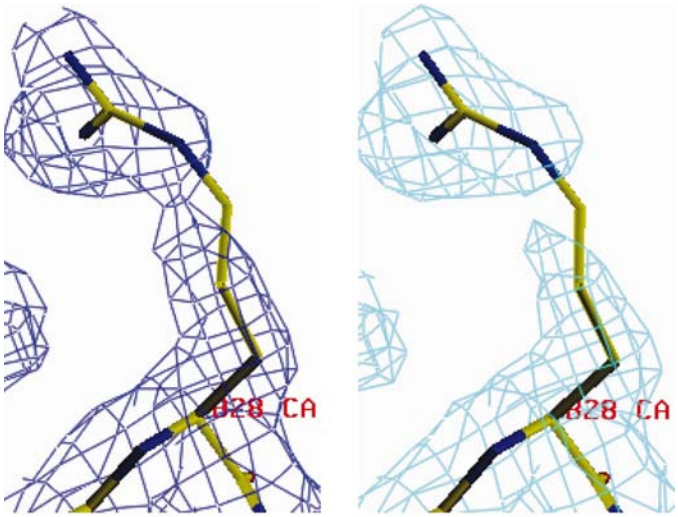

Figure 6
Section of $2F_o - F_c$ protein electron-density map using common reflections at 2 Å resolution showing Arg*B*28 at 1 r.m.s. contour level: (*a*) space data, for which the density is better, (*b*) earth data, for which the density is poorer. The map correlation coefficient for the side chain is 0.92 and 0.90, respectively, compared with the 1.85 Å space-grown crystal electron-density map.

Table 3
R.m.s. deviations.

	Space, 1.85 Å	Earth, 2 Å	Space, 2 Å (common)	Earth, 2 Å (common)
Space, 1.85 Å	—	0.122	0.166	0.139
Earth, 2 Å	0.122	—	0.148	0.120
Space, 2 Å (common)	0.166	0.148	—	0.075
Earth, 2 Å (common)	0.139	0.120	0.075	—

Table 4
Average temperature factors *B* (Å^2) for the four refined structures studied.

All values were determined using *BAVERAGE* (Collaborative Computational Project, Number 4, 1994).

	Protein only	Common waters only
Space crystal, 1.85 Å	20.9	28.8
Earth crystal, 2 Å	20.5	28.1
Space crystal, 2 Å, using common reflections with earth crystal	21.5	26.3
Earth crystal, 2 Å, using common reflections with space crystal	21.8	27.2

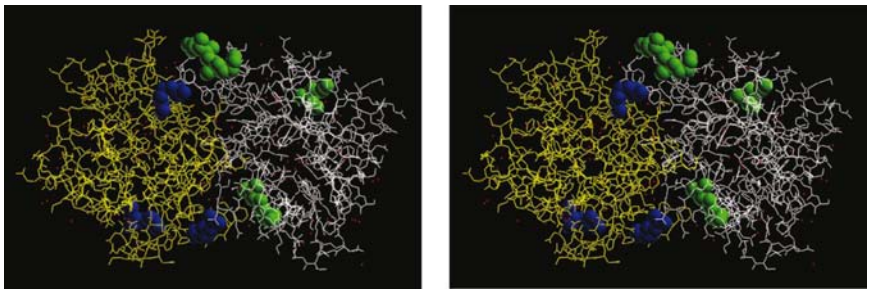

Figure 7
Stereoview of the molecule of apocrustacyanin C_1 with monomer *A* in white and monomer *B* in yellow. Seven residues are better in the space crystal when using common reflections at 2 Å resolution and these residues are shown as space-filled atoms in green and blue. These residues are Asp*A*1, Lys*A*2, Lys*A*19, Arg*A*79, Lys*B*2, Arg*B*28 and Glu*B*90; the improvements involve side chains for all except Lys*A*2, which involves its main chain. Residue Asp*A*1 is involved in crystal lattice-forming interactions, and Lys*A*2 nearby.

JH's salary was supported by The Leverhulme Trust. The European Synchrotron Radiation Facility ESRF in France is thanked for the provision of synchrotron radiation (BM14) under the auspices of an ESRF access arrangement set up by the European Space Agency (ESA). The space apocrustacyanin C_1 crystals were grown on a NASA Space Shuttle flight using the ESA APCF (Advanced Protein Crystallization Facility) *via* an award from ESA to NEC and PFZ. TJB was a Samuel Hall PhD student at the University of Manchester with JRH. Analysis of the structures was undertaken in the University of Manchester Laboratory of Structural Chemistry using the SG workstation suite originally funded by BBSRC and The Wellcome Trust, to whom JRH is also very grateful. JRH and JH are grateful to Dr Günter Grossmann of Daresbury Laboratory for discussions who asked 'Where are the improved amino-side chains located?' after a seminar given by JH on this research

References

Akker, F. van den & Hol, W. G. J. (1999). *Acta Cryst.* D**55**, 206–218.
Boggon, T. J. (1998). PhD thesis, Department of Chemistry, University of Manchester, pp. 195–209.
Boggon, T. J., Chayen, N. E., Snell, E. H., Dong, J., Lautenschloger, P., Potthast, L., Siddons, D. P., Stojanoff, V., Gordon, E., Thompson, A. W.,

Zagalsky, P. F., Bi, R.-C. & Helliwell, J. R. (1998). *Philos. Trans. R. Soc. London Ser. A*, **356**, 1045–1061.
Borgstahl, G. E. O., Vahedi-Faridi, A., Lovelace, J., Bellamy, H. D. & Snell, E. H. (2001). *Acta Cryst.* D**57**, 1204–1207.
Chayen, N. E, Boggon, T. J., Cassetta, A., Deacon, A., Gleichmann, T., Habash, J., Harrop, S. J., Helliwell, J. R., Nieh, Y. P., Peterson, M. R., Raftery, J., Snell, E. H., Hadener, A., Niemann, A. C., Siddons, D. P., Stojanoff, V., Thompson, A. W., Ursby, T. & Wulff, M. (1996). *Q. Rev. Biophys.* **29**, 227–278.
Chayen, N. E, Gordon, E. J. & Zagalsky, P. F. (1996). *Acta Cryst.* D**52**, 156–159.
Chayen, N. E, Snell, E. H., Helliwell, J. R. & Zagalsky, P. F. (1997). *J. Cryst. Growth*, **171**, 219–225.
Cianci, M., Rizkallah, P. J., Olczak, A., Raftery, J., Chayen, N. E., Zagalsky, P. F. & Helliwell, J. R. (2001). *Acta Cryst.* D**57**, 1219–1229.
Cianci, M., Rizkallah, P. J., Olczak, A., Raftery, J., Chayen, N. E., Zagalsky, P. F. & Helliwell, J. R. (2002). *Proc. Natl Acad. Sci. USA*, **99**, 9795–9800.
Collaborative Computational Project, Number 4 (1994). *Acta Cryst.* D**50**, 760–763.
Dong, J., Boggon, T. J., Chayen, N. E., Raftery, J., Bi, R.-C. & Helliwell, J. R. (1999). *Acta Cryst.* D**55**, 745–752.
Gordon, E. J., Leonard, G. A., McSweeney, S. & Zagalsky, P. F. (2001). *Acta Cryst.* D**57**, 1230–1237.
Jones, T. A., Zou, J. Y., Cowan, S. W. & Kjeldgaard, M. (1991). *Acta Cryst.* A**47**, 110–119.
Koszelak, S., Day, J., Leja, C., Cudney, R. & McPherson, A. (1995). *Biophys. J.* **69**, 13–19.
Kundrot, C. E., Judge, R. A., Pusey, M. L. & Snell, E. H. (2001). *Cryst. Growth Des.* **1**, 87–99.
Littke, W. & John, C. (1984). *Science*, **225**, 203–204.
McPherson, A. (1997). *Trends Biotechnol.* **15**, 197–200.
Ng, J. D., Sauter, C., Lorber, B., Kirkland, N., Arnez, J. & Giegé, R. (2002). *Acta Cryst.* D**58**, 645–652.
Otwinowski, Z. (1993). *Proceedings of the CCP4 Study Weekend. Data Collection and Processing*, edited by L. Sawyer, N. Isaacs & S. Bailey, pp. 56–62. Warrington: Daresbury Laboratory.
Otwinowski, Z. & Minor, W. (1997). *Methods Enzymol.* **276**, 307–326.
Smith, G. D., Ciszak, E. & Pangborn, W. (1996). *Protein Sci.* **5**, 1502–1511.
Snell, E. H., Cassetta, A., Helliwell, J. R., Boggon, T. J., Chayen, N. E, Weckert, E., Hölzer, K., Schroer, K., Gordon, E. J. & Zagalsky, P. F. (1997). *Acta Cryst.* D**53**, 231–239.
Snell, E. H., Weisgerber, S., Helliwell, J. R., Weckert, E., Holzer, K. & Schroer, K. (1995). *Acta Cryst.* D**51**, 1099–1102.
Vergara, A., Lorber, B., Zagari, A. & Giegé, R. (2003). *Acta Cryst.* D**59**, 2–15.
Walter, H. U. (1987). Editor. *Fluid Sciences and Materials Science in Space.* Berlin: Springer–Verlag.